World Academy of Science, Engineering and Technology
International Journal of Physical and Mathematical Sciences
Vol:8, No:9, 2014

An Investigation of New Phase Diagram of Ag_2SO_4 - $CaSO_4$

Ravi V. Joat, Pravin S. Bodke, Shradha S. Binani, S. S. Wasnik

Abstract**—**A phase diagram of the Ag_2SO_4 - $CaSO_4$ (Silver sulphate – Calcium Sulphate) binaries system using conductivity, XRD (X-Ray Diffraction Technique) and DTA (Differential Thermal Analysis) data is constructed. The eutectic reaction (liquid -» a-Ag_2SO_4 + $CaSO_4$) is observed at 10 mole% $CaSO_4$ and 645°C. Room temperature solid solubility limit up to 5.27 mole % of Ca^{2+} in Ag_2SO_4 is set using X-ray powder diffraction and scanning electron microscopy results. All compositions beyond this limit are two-phase mixtures below and above the transition temperature (≈ 416°C). The bulk conductivity, obtained following complex impedance spectroscopy, is found decreasing with increase in $CaSO_4$ content. Amongst other binary compositions, the 80$AgSO_4$-20$CaSO_4$ gave improved sinterability/packing density.

Keywords**—**Ag_2SO_4-$CaSO_4$ (Silver sulphate–Calcium Sulphate) binaries system, XRD (X-Ray Diffraction Technique) and DTA(Differential Thermal Analysis).

I. Introduction

THE sulphate based solid electrolytes have found potential application in electrochemical devices [1], [2]. Particularly, Li_2SO_4, Na_2SO_4 and Ag_2SO_4 based systems are potential materials from SO_X galvanic gas sensor viewpoint [2]. The first two materials have been studied extensively as compared to the latter one.

Amongst all the sulphates silver sulphate, a non-alkali metal is an exception that exhibits high Ag^+ conductivity. The high ionic conductivity, in spite of large' size of Ag^+ (1.26A°), has been suggested to be due to its high quadrapolar polarizability. The Ag_2SO_4 based solid electrolytes offer additional advantages from SO_X sensor application viewpoint [3]-[5]. Moreover, in these materials a major problem of cationic inter-diffusion between electrolyte and Ag-Ag_2SO_4 solid reference electrode does not remain valid for creating concentration gradients and so better long-term sensor operation stability [6]-[8].

Silver sulphate is a polymorphs compound. It undergoes a phase transition from the high temperature high conducting hexagonal α-phase (space group *p63/mmc)* to the low temperature moderately conducting orthorhombic β-phase (space group *Fddd)* at 418°C [9]. The latter phase is isomorphic with the low temperature form of Na_2SO_4 [10]. The electrical conductivity of pure Ag_2SO_4 has been investigated in 1967 by Kvist [11]. In 1990 Liu et al have measured the ionic conductivity of Me_2SO_4 (Me = Li, Na, and K) and MSO_4 (M = Sr, Ca and Ba) doped Ag_2SO_4 and subsequently, tested for their utility in the SO_2 gas sensor [12]. Electrical conductivity studies of mono-, di- and tri-valent cation doped Ag_2SO_4 have indicated that besides the valance of guest cation its size and electronic configuration also play important role in conductivity [13].

The multiphase sulphate based systems have been preferred in SO_2 gas sensor application due to their stable performance as compared to mono-phase. Moreover, the performance of sensor depends considerably on the magnitude of cationic conductivity, the phase and form along with the chemical and thermodynamical stability of solid electrolyte. Most of this information can easily be obtained from the binary-phase diagram and so they are important.

In 1907, Nacken has proposed the equilibrium phase diagrams of Ag_2SO_4 with mono-valent alkali sulphates (Me_2SO_4 where Me = Na and K) using the results obtained towards thermal analysis [14]. In a systematic study, Takahashi et al have initially determined the conductivity and later constructed the binary phase diagrams with silver halides (AgX- Ag_2SO_4, where X= Gland Br) with the help of transport number, differential thermal analysis and *x*-ray powder diffraction techniques [15]. A detailed investigation on Li_2SO_4 - Ag_2SO_4 binary phase diagram has been carried out by Oye [16]. Following an extensive work on Ag_2SO_4 - Me_2SO_4 (Me = Na and K) Secco et al., in recent past, have proposed Ag_2SO_4 - Rb_2SO_4 binary phase diagram [17], [18]. According to these phase diagram Ag_2SO_4 forms solid solution in entire compositional range of binary system. Whereas, in Li_2SO_4-Ag_2SO_4 system very limited two-phase region is available.

It is evident from the literature that so far a systematic investigation on the Ag_2SO_4 – MSO_4 (M = Sr, Ca, Ba) binary systems, which may be potential from SO_X gas sensor viewpoint, is lacking. All these factors have prompted us to investigate Ag_2SO_4 - $CaSO_4$ binary system, using electrical conductivity, differential scanning calorimetry, differential thermal analysis and x-ray powder diffraction techniques, constructing phase diagram to understand the phase and form of solid electrolyte belonging to this system in the vicinity of sensor operating temperature.

R. V. Joat is with the Department of Physics, Vidhya Bharati Mahavidyalaya, Amravati, PIN-444602, India (phone: +91-9422179298; e-mail: ravijoat@gmail.com).

P. S. Bodke is with the Department of Chemistry, Vidhya Bharati Mahavidyalaya, Amravati, PIN-444602, India (phone: +91-9823105999; e-mail: psbodke123@gmail.com).

S. S. Binani is with the Department of Chemistry, Vidhya Bharati Mahavidyalaya, Amravati, PIN- 444602, India (phone: +91-8055448934; e-mail: shradhabinani88@gmail.com).

S. S. Wasnik is with the Department of Physics, Vidhya Bharati Mahavidyalaya, Amravati, PIN- 444602, India.

II. Experimental

The initial ingredients Ag_2SO_4 and anhydrous $CaSO_4$ with purity greater than 99.9% were procured from E Merck. The above chemicals in (100-*x*) Ag_2SO_4 - (*x*) $CaSO_4$ (where *x,* -0.1, 2.5, 5.27, 7.57, 10, 20, ... 100) mole percent were mixed in an agate mortar under acetone for 2 hours. Well ground compositions were then transferred to translucent quartz ampoules and heated to the temperature 20°C above their respective melting point. The melt was allowed to cool, at the rate of 1.50°C min"[1], to room temperature. On the other hand, the compositions with more than 60-mole % of $CaSO_4$ were prepared by fusing the well ground mixture at 800°C in silica ampoules so as to avoid thermal decomposition of silver sulphate. The ingots obtained by breaking the ampoules were finally pulverized to get fine powder. The entire procedure was carried out in a dark room so as to avoid photodecomposition of silver sulphate.

All samples were characterized using X-ray powder diffraction (XRD) (Philips PW 1700 diffractometer attached with PW 1710 controlling unit) using CuKα radiation at room temperature. Whereas, XRD patterns were recorded at 300 and 450°C for *a* few selected samples viz. 20, 40 and 60 mole % $CaSO_4$ added to Ag_2SO_4. In order to set the room temperature solid solubility limit, diffraction patterns were recorded for 5.27 mol% $CaSO_4$ added to Ag_2SO_4 samples prepared by two different techniques viz. (i) initial ingredients Ag_2SO_4 and $CaSO_4$ in appropriate mole ratio were thoroughly mixed mechanically under acetone for 2 hours and (ii) melting the same thoroughly mixed composition followed by slow cooling the melt to room temperature. The information towards the solid-solid phase transition temperature, the melting point and the heat of transition were obtained by differential scanning calorimetry (DSC) and differential thermal analysis using Mettler TA 4000 DSC 25 and Mettler TA DTA, respectively (under inert atmosphere) at a cooling rate of 10 °C min"[1]. The microstructures were examined with the help of scanning electron microscope (SEM) (Cambridge 250 mark - III stereoscan electron microscope).

The bulk conductivity of all samples, at various temperatures, was obtained following complex impedance spectroscopy as described elsewhere [19], [20].

III. Results and Discussion

A. X-Ray Powder Diffraction (XRD)

A comparison of experimental *d* (Å) and relative intensity I/I_o of pure, $94.73Ag_2SO_4$-$5.27CaSO_4$, $93Ag_2SO_4$-$7CaS0_4$ and $90Ag_2SO_4$-$10CaSO_4$ with those of the JCPDS (joint committee for powder diffraction standards) data of Ag_2SO_4 and $CaSO_4$ is given in Table I. It is seen that experimental characteristic *d* lines of mechanically mixed samples match closely with those of the JCPDS data for Ag_2SO_4 and $CaSO_4$. On the other hand, all the experimental *d* values of $94.73Ag_2SO_4$-$5.27CaSO_4$ sample prepared by melting are found to be in close agreement with those of JCPDS data for Ag_2SO_4. No line(s) corresponding to $CaSO_4$ are seen in this composition. Similar results were found in the cases of $CaSO_4$ lower than 5.27 mole% added to Ag_2SO_4. A close look at the Table I reveals appearance of a few weak characteristic lines corresponding to $CaSO_4$ in case of $93Ag_2SO_4$-$7CaSO_4$. Furthermore, the number of characteristic lines due to $CaSO_4$ and their relative intensity are found to be increasing with increase in its concentration in Ag_2SO_4.

In the X-ray powder diffraction results of two-phase mixture, the relative intensity (I/I_0) values of each phase depend, more or less, on their concentration [21]. The absence of characteristic line(s) corresponding to $CaSO_4$ for $x = 5.27$ indicates the formation of a solid solution. Beyond this, all compositions are two-phase (β-Ag_2SO_4 + β-$CaSO_4$) mixtures. The absence of any unidentified peak(s) rules out the possibility of formation of an intermediate phase in the entire binary system.

Notably, the high temperature XRD results revealed bi-phase mixtures of β -Ag_2SO_4 + β -$CaSO_4$ and α-Ag_2SO_4 + β -$CaSO_4$ in the range from room temperature to 416°C and from 416 to 600°C, respectively. The lattice cell volume of Ag_2SO_4, within solid solubility limit, obtained from X-ray diffraction data is projected in Table II. As seen the cell volume decrease with increase in $CaSO_4$ concentration indicating lattice contraction (Ca^{2+} is smaller than Ag^+). These results endorse the formation of solid solution.

B. Scanning Electron Microscopy (SEM)

The microstructure of 10, 20 and 30 mol% $CaSO_4$ added to Ag_2SO_4 clearly indicate the formation of two-phase mixture and in $80Ag_2SO_4$ - $20CaSO_4$ it shows denser packing as compared to other compositions.

C. Thermal Analysis (DSC/DTA)

A typical DTA thermogram of $80Ag_2SO_4$-$20CaSO_4$ is depicted in Fig. 1. The solid-solid phase transition temperature and the melting point are obtained from the onset of endothermic peak. It is worth mentioning here that the values of T_c obtained following DSC and DTA analyses for all samples were found in agreement within the accuracy of ±2°C. Moreover, they were reproducible. A close look at the insert of Fig. 1 reveals a continuous decrease in the heat corresponding to solid-solid phase transition with an increase in $CaSO_4$ concentration in Ag_2SO_4. This is due to the decrease in net content of latter in the samples indicating formation of two-phase mixtures.

A phase diagram of Ag_2SO_4-$CaSO_4$ binary system, constructed using above XRD and DTA/DSC data is shown in Fig. 2. The solid circles represent the thermal discontinuities obtained from DTA/DSC. Thermodynamic features present in this binary system are summarized as follows, (a) the solid-solid phase transformation (α-Ag_2SO_4 → β-Ag_2SO_4) and melting point for Ag_2SO_4 are at 416 and 658°C, respectively, (b) the solid-solid phase transformation and melting point for $CaSO_4$ are at 1190 and 1450°C, respectively, (c) eutectic reaction (liquid → α-Ag_2SO_4 + $CaSO_4$) at 10 mole% $CaSO_4$ and 645°C (d) approximately 5 mole% $CaSO_4$ is soluble in β-$Ag2SO_4$ (e) two phase mixture of (β-Ag_2SO_4 + β-$CaSO_4$ exists between room temperature and 416°C, (f) two phase mixture

of α -Ag_2SO_4 + β -$CaSO_4$ exists between 416 and 655°JC for all compositions, (g) melt and solid β-$CaSO_4$ coexists beyond 30mole% $CaSO_4$ and above 655°C. Due to experimental limitation it was not possible to investigate thermal behaviour of samples above 1000°C. The dotted line is, however, an extrapolated liquidous curve.

A close look at this phase diagram reveals that T_c slightly decreases with an addition of $CaSO_4$ up to 7.5 mole% and thereafter it remains fairly constant. The initiatory decrease in T_c with an increase of $CaSO_4$ concentration is due to the formation of solid solution (Table I). Irvine and West have explained the decrease in T_c by assuming that the substitution of alio-valent cation results in the creation of extrinsic vacancies that causes lattice distortion/disorder [22]. According to them, the order-disorder phase transition in solid solution occurs more readily with rising temperature, and T_c displaces to a lower temperature.

D. Temperature Dependent Conductivity

The plots of log (σT) versus $10^3/T$ for (x)Ag_2SO_4: (l-x)$CaSO_4$ system for x = 0-10, v = 10-60 and x = 70-100 mole% are displayed in Figs. 3, 4 (a) and 4 (b), respectively. As seen, in both orthorhombic (stable below 416 °C) and hexagonal (stable above 416°C) modifications of Ag_2SO_4 conductivity obey the Arrhenius law.

Observed change in conductivity at 416°C, for all samples, accounts for orthorhombic (β) to hexagonal *(α)* phase transition in Ag_2SO_4. Notably, this temperature coincides with the T_c obtained from DSC and DTA investigations. The change in slop in conductivity plot around 416°C, ascribed to switch in conduction mechanism due to structural phase-transition, is the manifestation of partial insolubility of $CaSO_4$ in Ag_2SO_4 and vice-versa. Also, it rules out the formation of new intermediate compound in the entire binary system. These results are in agreement with above discussed XRD and DTA results. The conductivity measurements were restricted to below 560°C due to softening/deformation of samples at this temperature.

Insert of Figs. 3, 4 (a) and 4 (b**)** display the conductivity behavior (in both the modifications) of samples with $CaSO_4$ addition. In the high temperature modification (Fig. 3), the conductivity exhibits a maximum at 7.57 mole% (≈ 7% vacancies) $CaSO_4$ within the solid solubility region. Whereas, in two-phase region (Figs. 4 (a) and (b)), it remains fairly invariant. In contrast, the conductivity below the transition temperature decreases (insert of Figs. 3, 4 (a) and 4 (b)).

The maximum in conductivity at 7.57 mole%, corresponding to ≈ 7% vacancies, is in good agreement with the reporting [23]. Since Ca^{2+} (0.99A) is smaller than Ag^+ (1 .26 A), the partial replacement of latter by former leads to an appreciable lattice contraction (Table II) in room temperature phase of Ag_2SO_4. Hence, Ca^{2+} addition gives an additional vacancy with deeper potential well that offers large activation energy for Ag^+ migration. Therefore, as $CaSO_4$ content increases, conductivity decreases in low temperature phase.

TABLE I
A COMPARISON OF EXPERIMENTAL X-RAY DIFFRACTION LINES WITH JCPDS FOR 5.27, 7 AND 1JO MOLE % CASO4 ADDED TO AG_2SO_4

Mechanical Mixed				Melt slow cooled				JCPDS		
5.27mole% Ca		5.27mole%Ca		7mole% Ca		10 mole% Ca				
d	*I/I₀*	*d*	*I/I₀*	*d*	*I/I₀*	*d*	*I/I₀*	*d*	*I/I₀*	Phase (hlk)
4.72	7	4.72	10	4.73	10	4.61	9	4.70	10	Ag_2S0_4(lll)
4.00	8	3.99	23	4.01	20	3.95	21	3.99	25	Ag_2S0_4(220)
3.51	25	--	—	3.51	13	3.40	19	3.49	100	$CaSO_4$(002)
3.18	48	3.18	76	3.18	85	3.15	82	3.17	10	$A_{g2}S0_4$(040)
2.87	100	2.87	100	2.88	100	2.92	100	2.87	100	Ag_2S0_4(311)
2.65	36	2.65	68	2.65	64	2.54	78	2.64	90	$A_{g2}S0_4$(022)
2.53	13	2.53	12	2.53	13	2.53	14	2.53	17	Ag_2S0_4(202)
2.42	11	2.42	26	2.43	21	2.42	25	2.42	30	Ag_2S0_4(033)
2.27	4	2.27	6	2.27	8	2.26	5	2.27	8	Ag_2S0_4(151)
2.20	6	--	—	2.20	1	2.20	4	2.20	20	$CaSO_4$(212)
2.18	5	--	—	2.18	6	2.19	8	2.18	8	CaSO4
1.98	5	1.98	8	1.98	6	1.97	8	1.98	11	$A_{g2}S0_4$ (242)
1.95	4	--	—	1.95	5	1.94	7	1.95	8	Ag_2SO_4 (260)
1.93	2	--	—	1.93	7	1.93	9	1.94	4	$CaSO_4$ (222)
1.92	14	1.92	34	1.92	23	1.92	20	1.92	30	Ag(351)
1.88	4	1.87	5	1.88	3	1.88	4	1.88	5	Ag(H3)
1.74	2	--	—	1.74	3	1.69	6	1.74	10	$CaSO_4$ (040)
1.71	9	1.71	13	1.71	12	1.75	13	1.71	17	Ag?$S0_4$ (062)

JCPDS card No. 27-1403 (Ag_2SO_4) ad 6-0226 ($CaSO_4$)

TABLE II
COMPARISON OF EXPERIMENTAL LATTICE CELL CONSTANTS WITH JCPDS

Cell constants	JCPDS (Ag_2S0_4)[a]	$CaS0_4$ doped Ag_2SO_4		
		x = 00	x = 0. 05	x = 0.0527
a (A)	10.2699	10.247	10.268	10.252
b (A)	12.7069	12.693	12.679	12.625
c (A)	759.25	758.32	758.32	740.08

JCPDS card number 27-1403 (Ag_2SO_4).

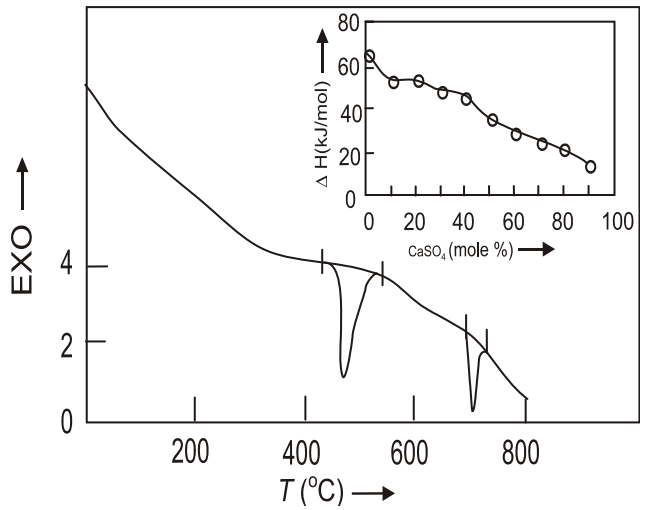

Fig. 1 DTA thermogram of 80 Ag_2SO_4-20$CaSO_4$ and insert variation of phase transition enthalpy with the addition of $CaSO_4$ in Ag_2SO_4

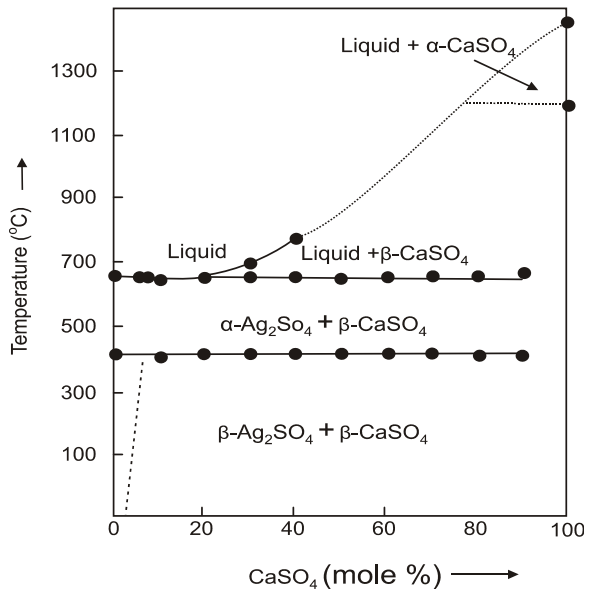

Fig. 2 The phase diagram for Ag_2SO_4–$CaSO_4$ binary system The solid circles represent thermal discontinuity as determined from differential thermal analysis. The indicated bi-phase regions are confirmed by x-ray diffraction. The broken line near Ag_2SO_4 end indicates the uncertainty of the solid solution range in this phase. The dotted line is expected liquidous curve

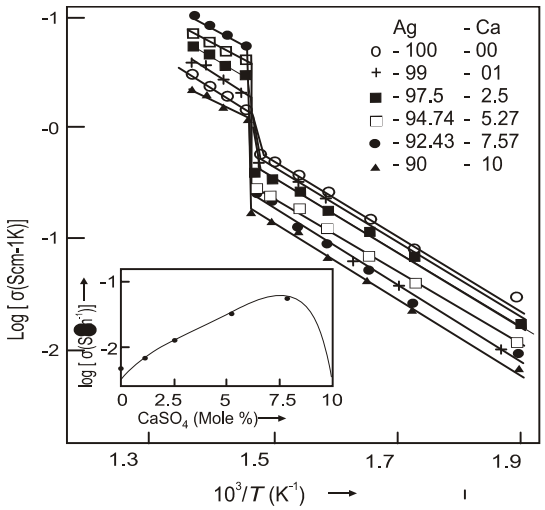

Fig. 3 log (σT) versus 1000/T for (l-x) Ag_2SO_4 - (x) $CaSO_4$ where x = 0 - 10 .Insert indicates the variation of conductivity with CaSO4 concentration

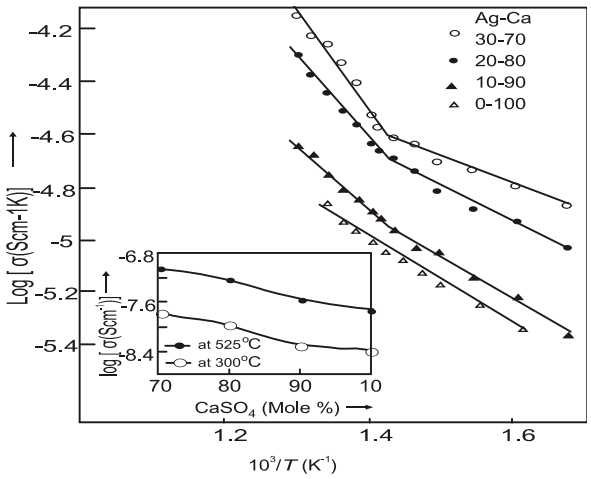

(a)

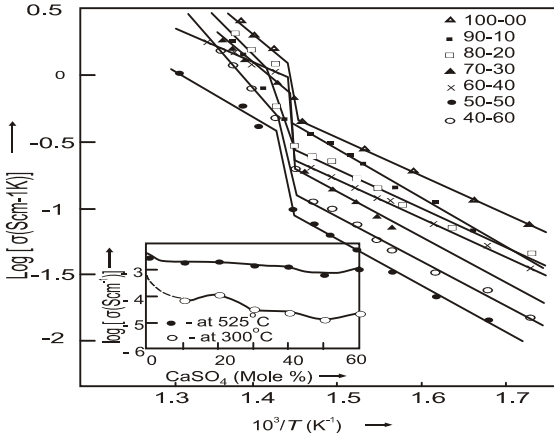

(b)

Fig. 4 (a) log (σT) versus 1000/ T for (1 -x) Ag_2SO_4 - (x) $CaSO_4$ binary system with (a) x = 10-60 and (b) x = 70 -100. Insert indicates variation of conductivity with $CaSO_4$ concentration

IV. Conclusion

The $CaSO_4$ is sparingly soluble in both the hexagonal and the orthorhombic phases of Ag_2SO_4 and form bi-phase mixtures in entire binary system. The eutectic reaction (liquid → α-Ag_2SO_4 + $CaS0_4$) is observed at 10 mole% $CaSO_4$ and 645°C. The value of conductivity although decreased but 20 mole % $CaSO_4$ added to $AgSO_4$ is useful for Sox gas sensor application due to (i) its bi-phase nature at operating temperature, (ii) low activation enthalpy for ion migration, (iii) improved sinterability and (iv) good mechanical strength.

Acknowledgment

Authors are thankful to the Principal, Vidyabharati Mahavidyalaya, Amravati for providing the laboratory facilities.

References

[1] B. Heed, A. Lunden and K. Schroeder, 10th Intersoc Energy Conversion Engg. Conf,Aug(1975)p.613.
[2] K, Singh and S. S. Bhoga, Bull Mater. Sci., 22 (1999) 71.
[3] Q. G. Liu and W. L. Worrel, U.S. Pat, 303-320 (1981) 17.
[4] W. L. Worrel and Q. G. Liu, J. Electroanal. Chem., 168 (1984) 355.
[5] C. M. Mari," M. Beghi and S. Pizrini, Sensors and Actuators B, 2 (1990) 51.
[6] H. Flood and N. Boye, Z. Electrochem., 66 (1962) 184.
[7] D. M. Haaland, J. Electrochem. Soc., 127 (1980) 796.
[8] Y. Saito, T. Maruyama, Y. Matsumoto, K. Kobayashi and Y. Yan, Solid State Ionics, 14(1984)273.
[9] M. Kumari, E.A. Secco, Can. J. Chem. 56 (1978) 2616.
[10] Y. Saito, T. Maruyama, Y. Matsumoto, K. Kobayashi, Thermochim Acta, 53 (1982) 289.
[11] A. Kvist, Acta Universitat, Gothoburgensis 2 (1967).
[12] Q. Liu, X. Sun and W. Wu, Solid State Ionics, 40-41 (1990) 465.
[13] K. Singh, S. M. Pande, S. W. Anwane and S. S. Bhoga, J. Appl. Phys. A, 66(1998) 205.
[14] R. Nacken, Neues Jahrb. Mineral. Geol, 24 (1907) 55.
[15] T. Takahashi, E. Namura and O. Yamamoto, J. Appl. Electrochem, 2 (1972) 51.
[16] H. A. Oye, Thesis (Technical University of Norway, Trondheim) 1963.
[17] M. S. Kumari and E. A. Secco, Can. J. Chem. 61 (1983) 2804.
[18] M. S. Kumari and E. A. Secco, Can. J. Chem. 63 (1985) 324.
[19] K. Singh and S. S. Bhoga, Appl. Phys. A. 67 (1998) 475.
[20] K Singh and S. S. Bhoga, *Proc. 4th National Seminar on Physics and Technology of Sensors,* India, (1997) C23-.
[21] K. Singh and S. S. Bhoga, J. Solid State Chem., 97 (1992) 141.
[22] T. S. Irvin and A. R. West, Solid State Ionics. 28 (1988) 214.
[23] H. H. Hoffer, W. Eysel and U. V. Alpen, J. Solid State Chem., 36 (198\1) 365.